



Dynamic Adaptive Impedance Matching in Magnetic Coupling Resonant Wireless Power Transfer System

Qiang Zhao^(✉)  and Chang Cui

School of Information and Control Engineering, Liaoning Shihua University,
Fushun 113001, China
lnshzq@126.com

Abstract. The circuit and environment of Wireless Power Transfer (WPT) system are always complex, which makes it difficult to design the magnetic coupler and reduce the transmission efficiency. Recently, a few advanced matching strategies and structures have been able to improve transmission efficiency in the WPT system when the magnetic coupling system is detuning. But the current compensation and matching system suffers from difficulties in optimization and generalization. To address this issue, in the present work, an external coupling modeling and adaptive dynamic impedance matching method are applied to the energy transmission optimization for WPT system. Firstly, an external coupling network modeling method is designed in a four-coil magnetic coupling resonance system, and a scattering parameter expression method of T-type network transmission efficiency is defined. Secondly, we add frequency independent compensation reactance to the circuit, and use external coupling coefficient to match the impedance of the system to eliminate the detuning and improve the transmission efficiency. Tertiary, the frequency independent impedance is realized by using controllable capacitance, and the value range of compensation capacitance is determined. Finally, experiments and simulations show that the optimized system has good impedance matching and transmission efficiency.

Keywords: Wireless energy transfer · Impedance matching · External coupling · Scattering parameters · Dynamic compensation

1 Introduction

Wireless power transfer (WPT) mainly realizes the energy transmission through non-contact way, which is a new mode for electrical equipment to obtain electric energy from the fixed grid system [1–3]. Its appearance has completely changed the mode that people only rely on the contact type electric energy conduction mode of electrical equipment for hundreds of years. It is also a hot topic of human research. At present, wireless power supply technology has been widely used in many fields, such as household appliances, convenient equipment, vehicles, aerospace, medical devices, industrial robots, oil fields and mines, underwater operations, etc. [4–6]. Compared with the traditional power supply technology, wireless energy transmission technology has the advantages of high

security, stable operation, low failure rate, suitable for various environments, conducive to the standardization of the interface, easy to achieve automation and unmanned operation, convenient maintenance and other advantages [7].

WPT technology is the most active research direction in the field of electrical engineering at present. It is an interdisciplinary research field integrating electromagnetic field, power electronic technology, physics, materials science, circuit and other disciplines. It has a broad development prospect [8]. The research of this subject has important scientific significance, high practical value and broad application prospect, which can bring huge economic and social benefits. Therefore, WPT will become the latest significant research direction in the field of modern industrial automation, which is important for accelerating the development of high-end equipment manufacturing industry, energy conservation and environmental protection, promoting industrial upgrading Meaning [9].

With the in-depth study of the magnetic coupling resonance WPT technology, there are still many problems in the development process of the technology, including coupling coefficient [10], frequency stability in the process of energy transmission and frequency bifurcation phenomenon [11], system structure optimization [12], multi-resonance network compensation [13], electro-magnetic compatibility [14], impedance matching and transmission power [15, 16], which are urgent to be solved.

For the WPT system, the influence of circuit parameters on the resonance frequency of the system and how to solve the influence caused by the relative position change between coils are all the problems faced by the research on the mechanism of magnetic coupling resonance WPT. It mainly involves resonance compensation, frequency splitting, impedance matching, dislocation coupling and other key issues [17]. Impedance matching is the core problem in the magnetic coupling resonance system. The research on system structure, transmission characteristics and frequency splitting are focused on impedance matching [18]. In the radio energy transmission system, the reflection impedance, the parasitic resistance of the coil, the source impedance and the load impedance constitute a complex impedance network, which has an important impact on the transmission characteristics of the system [19].

In order to improve the transmission power of the system, a new matching structure is proposed in [20]. In the transmitter, the series/parallel capacitor matrix can be dynamically matched by changing the combination matrix impedance of the series and parallel capacitors of the capacitor Tracking the best impedance matching point at different distances. In [21], according to the load change of multi coil radio energy transmission system, the system network is impedance matched by capacitance. The influence of different matching structures on the system performance is analyzed when the load and cross coupling relationship change. In [22], multi capacitor topology is adopted to reduce the influence of distance variation on the input impedance of the system. According to the input return loss, an adjustable impedance matching circuit and an optimization algorithm are designed. The experimental results show that the designed impedance matching circuit can achieve high-efficiency power transmission when the transmission distance changes in a large range. Multiple impedance matching networks of shunt switchable capacitors are added to the transmitter, and the coupling relationship is adjusted by adjusting each shunt capacitor. The performance of multi load power transmission is improved in [23]. A new adaptive impedance matching

network is proposed in [24], which is automatically reconfigured to keep the matching with the coil and adjust the output power to adapt to the change of coil distance. The closed-loop control algorithm is used to continuously change the capacitor, which can compensate the mismatch and adjust the output power at the same time. Compared with the system without matching, when the coupling coefficient is 0.05-0.8, the power transfer efficiency of the system is improved by 31.79% and 60%. [25] discussed a new design method of matching circuit based on genetic algorithm and random measurement of S parameters of moving coil. It can further simplify the simulation of matching circuit design and derive the optimal matching circuit.

In this work, we investigate a method of dynamic impedance matching in the wireless power transfer. A matching control method with controllable capacitance compensation is introduced to reduce the transmission efficiency caused by the system detuning. A two-port network analysis model based on external coupling network is established, and a frequency independent controllable compensation reactance is introduced into the resonant circuit. The half bridge circuit is used to realize the controllable compensation capacitance, and determined the value range of the compensation capacitance.

2 Magnetically Coupled Resonators Model

In the four-coil magnetically coupled resonant system shown in Fig. 1.

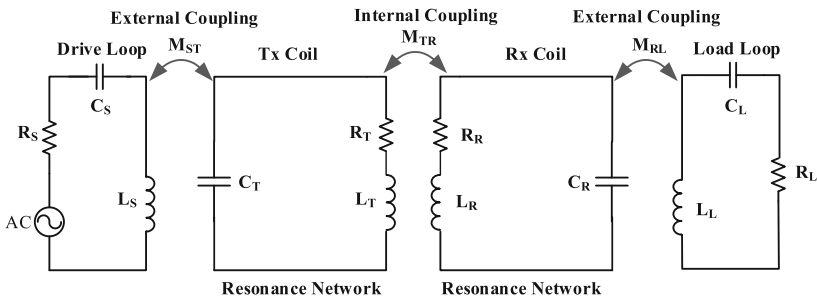


Fig. 1. Equivalent circuit model of four coils wireless power transmission.

In Fig. 1, M_{ST} and M_{RL} are the mutual inductance between the external and the internal resonant network, and the M_{TR} is the mutual inductance of the internal resonance. The excitation and the pick coil constitute an external resonant network. The transmit and receive coils constitute an internal resonant network. The high-frequency electric power source drives the excitation coil to generate a high-frequency oscillating magnetic field, which can be transmitted to the internal LC network by external coupling to resonate. The internal transmit coil and receive coil are internally coupled with each other to form contactless electrical energy transmission. As the internal resonant network and external resonant network using magnetic coupling method for energy

transmission, so the use of coil mutual inductance as a parameter to establish T-type equivalent impedance conversion network circuit model, as shown in Fig. 2.

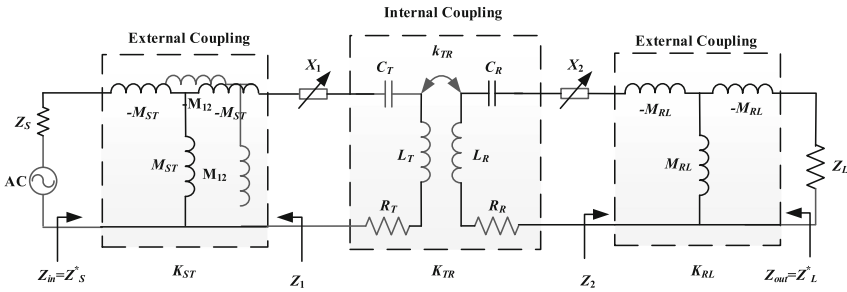


Fig. 2. Equivalent impedance conversion two-port network circuit model.

In Fig. 2, $Z_S = R_S + j\omega L_S + 1/j\omega C_S$, $Z_L = R_L + j\omega L_L + 1/j\omega C_L$, K_{ST} , K_{RL} are the equivalent impedance transform network of the external resonant network, and K_{TR} is the equivalent impedance transformation network of the internal resonant network, which is only related to the coupling coefficient k_{TR} between the two coils. The internally coupled two-port network transfer parameter matrix can be expressed as follow:

$$T_{TR} = \begin{bmatrix} A_{TR} & B_{TR} \\ C_{TR} & D_{TR} \end{bmatrix} \tag{1}$$

Where, $A_{TR} = Z_T/j\omega M_{TR}$, $B_{TR} = (Z_T Z_R/j\omega M_{TR}) - j\omega M_{TR}$, $C_{TR} = 1/j\omega M_{TR}$, $D_{TR} = Z_R/j\omega M_{TR}$, $Z_T = R_T + j\omega L_T + 1/(j\omega C_T) \pm jX_1$, $Z_R = R_R + j\omega L_R + 1/(j\omega C_R) \pm jX_2$

The external equivalent impedance transform two-port network transfer parameter matrix can be expressed respectively as follow:

$$T_{ST} = \begin{bmatrix} A_{ST} & B_{ST} \\ C_{ST} & D_{ST} \end{bmatrix} = \begin{bmatrix} 0 & -j\omega M_{ST} \\ 1/j\omega M_{ST} & 0 \end{bmatrix} \tag{2}$$

$$T_{RL} = \begin{bmatrix} A_{RL} & B_{RL} \\ C_{RL} & D_{RL} \end{bmatrix} = \begin{bmatrix} 0 & -j\omega M_{RL} \\ 1/j\omega M_{RL} & 0 \end{bmatrix} \tag{3}$$

In Fig. 2, the external and internal coupling networks are cascaded to form a new two-port network. According to the cascade characteristic of the two-port network, the total transmission parameters after cascade are shown in (4).

$$T = T_{ST} \times T_{TR} \times T_{RL} = \begin{bmatrix} A & B \\ C & D \end{bmatrix} \tag{4}$$

Where, the total transmission parameters are

$$A = (A_{ST}A_{TR} + B_{ST}C_{TR})A_{RL} + (A_{ST}B_{TR} + B_{ST}D_{TR}) C_{RL}$$

$$\begin{aligned}
 B &= (A_{ST}A_{TR} + B_{ST}C_{TR})B_{RL} + (A_{ST}B_{TR} + B_{ST}D_{TR}) D_{RL} \\
 C &= (C_{ST}A_{TR} + D_{ST}C_{TR})A_{RL} + (C_{ST}B_{TR} + D_{ST}B_{TR}) C_{RL} \\
 D &= (C_{ST}A_{TR} + D_{ST}C_{TR})B_{RL} + (C_{ST}B_{TR} + D_{ST}B_{TR}) D_{RL}
 \end{aligned}$$

The WPT system as the two-port network with one port being input fed by the source and the other being output fed by the load. Based on the scattering parameter, the transfer efficiency will be represented in terms of the linear magnitude of the scattering parameter $|S_{21}|$, the function of power transfer efficiency is defined as $\eta = |S_{21}|^2$ when the network is matching at both ports, in which $|S_{21}|$ is given by

$$S_{21} = 2 \frac{V_S}{V_L} \sqrt{\frac{Z_S}{Z_L}} \quad (5)$$

Where, V_S power voltage, V_L load voltage, Z_S power impedance, Z_L load impedance.

Assuming that the port impedance $Z_S = Z_L = Z_P$, S_{21} can be expressed as a T parameter.

$$S_{21} = \frac{2}{A + B/Z_P + CZ_P + D} \quad (6)$$

$$\eta = |S_{21}|^2 = \frac{4}{(A + B/Z_P + CZ_P + D)^2} \quad (7)$$

From the system efficiency in (7), the system efficiency is a function of the port impedances Z_S , Z_L and the transmission parameters A , B , C , D , when the system port impedance value is fixed, the system efficiency is only related to the transmission parameters.

3 Optimization of Magnetic Coupled Resonant Network

Only two levels of headings should be numbered. Input impedance Z_{in} of external coupling network after adding impedance matching circuit is

$$Z_{in} = R_{in} + jX_{in} = \frac{K_{ip}^2}{Z_P} \quad (8)$$

In (8), Z_P is the impedance of power or load port, K_{ip} is the coupling impedance transformation network connecting internal resonance circuit and external port.

It can be seen from (8) that the port impedance Z_P of the equivalent impedance transform network is represented by the input impedance Z_{in} and the characteristic impedance K_{ip} causes the phase shift $\pm 90^\circ$ between the two impedances. The corresponding two-port transfer parameter matrix of (8) can be expressed as

$$\begin{bmatrix} A_{ip} & B_{ip} \\ C_{ip} & D_{ip} \end{bmatrix} = \begin{bmatrix} 0 & \pm jK_{ip} \\ \mp \frac{j}{K_{ip}} & 0 \end{bmatrix} \tag{9}$$

Comparing (8) and (9) can be obtained $K_{ip} = \omega M_{ip}$, therefore, the characteristic impedance K_{ip} can be used to adjust the equivalent impedance of the two-port equivalent circuit of T-type mutual inductance, and the impedance transformation process of the network is shown in Fig. 3.

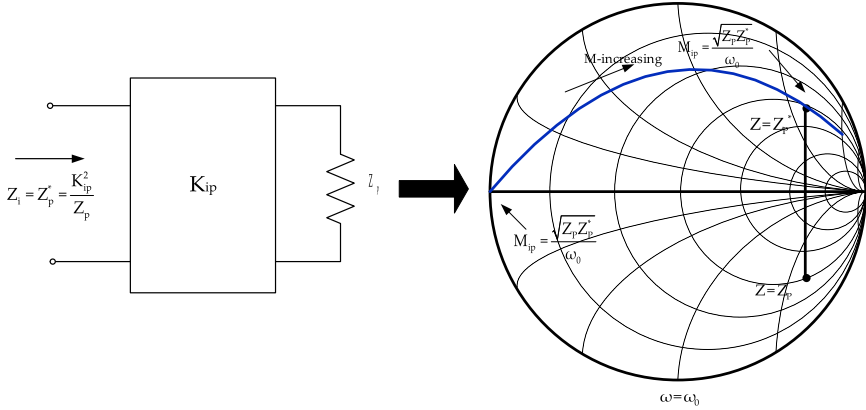


Fig. 3. Input impedance tracking process for coil inductance change in resonant state.

It can be seen from the Smith chart in Fig. 3 that the input impedance and the load impedance are symmetrical about the real axis when $M_{ip} = \sqrt{Z_p Z_p^*} / \omega_0$.

Substituting the port impedance Z_p into (8) can be rewritten as

$$Z_{in} = \frac{K_{ip}^2}{Z_p} = \frac{K_{ip}^2 R_p}{|Z_p|^2} - j \frac{K_{ip}^2 X_p}{|Z_p|^2} \tag{10}$$

As the resonance frequency ω_{0i} is a function of reactance, the reactance part $K_{ip}^2/X_p |Z_p|^2$ in the coupling impedance transformation network will make the working frequency of the circuit deviate from the resonance frequency, which will cause the system detuning and reduce the power transmission efficiency. In order to counteract the reactance that causes the system to be detuned, it is necessary to introduce a frequency-independent controllable reactive reactance X_i in the resonant circuit as shown in (11).

$$X_i = -\text{Im}(Z_i) = \frac{K_{ip}^2 X_p}{|Z_p|^2} = \frac{\omega^2 M_{ip}^2 X_p}{|Z_p|^2} \tag{11}$$

From (11), when the port parameters and ω are constant, the controllable compensating reactance is a function of the externally coupled mutual inductance M . The equivalent impedance K_{ip} of transmission network changes with external coupling. By adjusting the controllable compensation reactance X_i to the matching value, even if it meets the formula (11), for a given port impedance, the network parameters can be configured to prevent the occurrence of detuning. By substituting the parameters related to the transmission efficiency of the system into (6), we can get

$$\begin{aligned}
 S_{21}|_{\omega=\omega_0} &= 2j \frac{k_{TR} \frac{k_p^2}{\omega_0 L_i R_p}}{[-k_{TR}^2 + (\frac{k_p^2 X_p}{\omega_0 L_i |Z_p|^2} - \frac{j}{Q_i})^2](-j + \frac{X_p}{R_p})^2 - 2 \frac{k_p^2}{\omega_0 L_i R_p} (\frac{k_p^2 X_p}{\omega_0 L_i |Z_p|^2} - \frac{j}{Q_i})(-j + \frac{X_p}{R_p}) + \frac{k_p^4}{(\omega_0 L_i R_p)^2}} \\
 &= 2j \frac{k_{TR} \frac{k_p^2}{\omega_0 L_i R_p}}{-k_{TR}^2(-j + \frac{X_p}{R_p})^2 + [\frac{k_p^2}{\omega_0 L_i R_p} - (\frac{k_p^2 X_p}{\omega_0 L_i |Z_p|^2} - \frac{j}{Q_i})(-j + \frac{X_p}{R_p})]^2}
 \end{aligned} \tag{12}$$

Under the given parameters, the (13) is derived as follow.

$$\left. \frac{\partial S_{21}}{\partial k_p} \right|_{\omega=\omega_0} = 0 \tag{13}$$

The optimal value of k_p when the maximum transmission efficiency is obtained is

$$k_{p-opt} = \left(1 + k_{TR-opt}^2 Q_i^2\right)^{1/4} |z_p| \sqrt{\frac{R_i}{R_p}} \tag{14}$$

In (14), the port impedance and resonance quality factor are fixed values, and the optimized value of internal coupling factor K_{p-opt} is determined by the distance and position of resonance coil.

The impedance matching and resonance compensation of the system can be easily realized by using the impedance variation characteristic and the transmission response and power transmission efficiency of the system can be optimized.

Half-bridge controllable compensation reactance model shown in Fig. 4, the circuit consists of two full-control switches (V_{T1} , V_{T2}) with capacitor in parallel, and the capacitance voltage is

$$u_{CT} = U_{CT} \sin(\omega t) \tag{15}$$

The initial voltage on the capacitor is zero, V_{T1} and V_{T2} are in inverse series and the trigger signal is the same. Trigger angle range is $90^\circ < a < 180^\circ$, while the trigger signal on the voltage zero-point symmetry, conduction angle is $\pi - \alpha$.

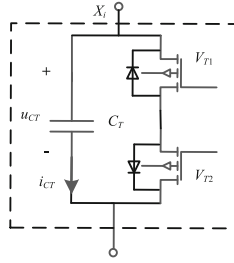


Fig. 4. Half-bridge controllable compensation reactance model.

The voltage of capacitor branch during conduction of V_{T1} or V_{T2} is as follows.

$$u_{CT}(t) = \int_{\alpha}^{\omega t} \frac{1}{\omega C_T} i_{CT}(t) dt = \int_{\alpha}^{\omega t} \frac{1}{\omega C_T} (\sqrt{2}I \cos \omega t) dt \tag{16}$$

$$\omega t = \alpha + k\pi \quad (k = 0, 1, 2, \dots)$$

The u_{CT} is expanded by Fourier series, and only the fundamental wave term is retained as shown in (17).

$$u_{CT} = \frac{2}{\sqrt{2}\pi} \int_0^{\pi} [u_{CT}(\omega t) * \sin \omega t] dt$$

$$= \frac{\sqrt{2}}{\pi} \int_{\alpha}^{\pi-\alpha} \left\{ \left[\sqrt{2}I \frac{1}{\omega C_T} (\sin \omega t - \sin \alpha) \right] \sin \omega t \right\} dt \tag{17}$$

$$= I \frac{1}{\omega C_T} \left(1 - \frac{2\alpha}{\pi} - \frac{2 \sin 2\alpha}{\pi} \right)$$

From (17), the equivalent capacitor can be solved as follow:

$$C_{eq} = \frac{\pi C_T}{\pi - 2\alpha - 2 \sin 2\alpha} \tag{18}$$

Therefore, the controllable compensation reactance value can be expressed as:

$$X_i = \frac{1}{\omega C_{eq}} = \frac{\pi - 2\alpha - 2 \sin 2\alpha}{\pi \omega C_T} \tag{19}$$

The controllable compensation reactance can be adjusted continuously in a certain range by changing the trigger angle α . The adjustable reactance is used to compensate the reactance which causes the system detuning in the coupling impedance transformation network, and a variable reactance and reactive power compensation with a variation range of $0-X_c$ is realized.

In the WPT system, the main compensation in the circuit is the port impedance and the inductive reactive power component in the impedance transformation network. Therefore, the range of values for C_{eq} is as follows.

$$\min\left(\frac{|Z_p|^2}{\omega K_{ip}^2 X_p}\right) < C_{eq} < \max\left(\frac{|Z_p|^2}{\omega K_{ip}^2 X_p}\right) \tag{20}$$

According to the adjustment range ($\alpha_{min}, \alpha_{max}$) of trigger angle, the range of controllable compensation reactance can be calculated as (X_{i-min}, X_{i-max}).

4 Experimental and Result Analysis

In order to verify the feasibility of the above adaptive tuning method, simulation and experimental verification are carried out. The transmitter and receiver of the system are tuned in tow-sides. The system parameters are shown in Table 1.

Table 1. Detailed parameter values of coils.

Parameters	Symbol	Value
Turns of Tx and Rx coils	N_i	5
Turns of excitation and pickup coils	N_p	1
Outer diameter of Tx and Rx coils	D_{i-max}	300 mm
Inner diameter of Tx and Rx coils	D_{i-min}	200 mm
Diameter of excitation and pickup coils	D_p	180 mm
Coil turn spacing	p	17 mm
Wire diameter	$r_i = r_p$	3 mm
Coil distance	d_{23}	0 ~ 1500 mm

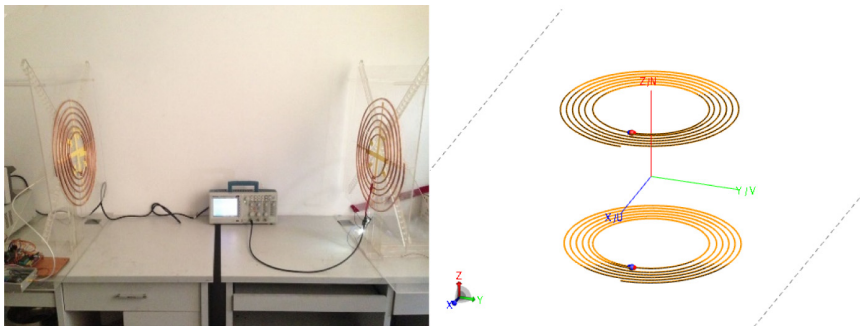


Fig. 5. Simulation model and experimental device of magnetically coupled resonant coil.

Simulation model and experimental device of magnetically coupled resonant coil as shown in Fig. 5.

In the experimental device, the plane spiral coils are made of hollow copper tube. The excitation and the transmitting coil have the same center, and the receiving and picking coils have the same structure. Class E amplifier is used as high frequency inverter to connect excitation coil and programmable electronic load to connect pick-up coil. The operating frequency of the system is 12–15 MHz. The simulation analysis of the plane spiral coil system is carried out. When the transmission distance is 600 mm, the scattering parameter curve of the system is shown in Fig. 6.

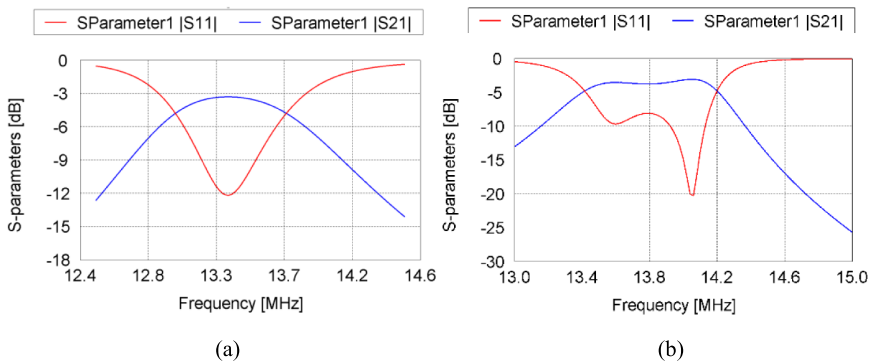


Fig. 6. S Parameter before and after optimization of 400 mm transmission distance (a) The original WPT system (b) The optimized WPT system.

As shown in Fig. 6, after optimization, the forward transmission coefficient of the system is larger and has two resonance frequency points, while the original WPT system is only one, and the maximum value of -3 dB is not reached. After optimization, the reflection coefficient of the input port of the system is obviously reduced, which shows that the transmission capacity of the system is significantly improved. The impedance matching method is used to optimize the system, the resonant frequency of the coil is rematches to the power frequency (14.1 MHz), and the frequency split is eliminated. The optimized current of port is shown in Fig. 7.

As can be seen from Fig. 7, the input and output port of the low frequency point have the same current polarity, while the high frequency resonance point has the opposite polarity. Although the polarity of the two ports before optimization is opposite at both frequency points, the current distribution does not have obvious frequency division phenomenon, and the current after optimization has been significantly improved.

The input impedance of the wireless power transmission system plays an important role in the analysis of transmission characteristics, as shown in Fig. 8.

It can be seen from Fig. 8 that the optimized input impedance is larger and has better load performance in general, so that the system has better transmission characteristics.

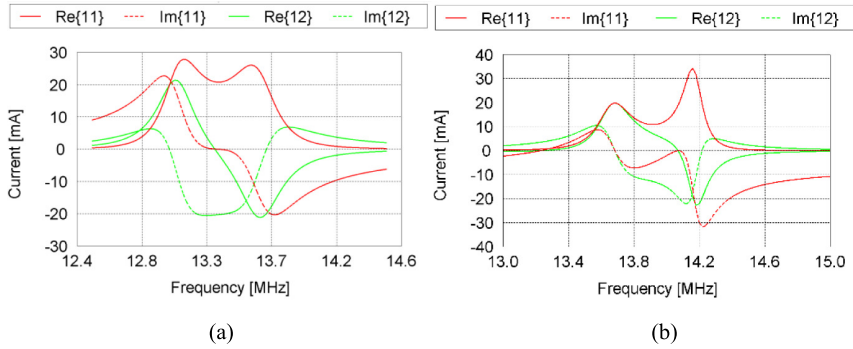


Fig. 7. The optimized current of input and output port (a) The original WPT system (b) The optimized WPT system.

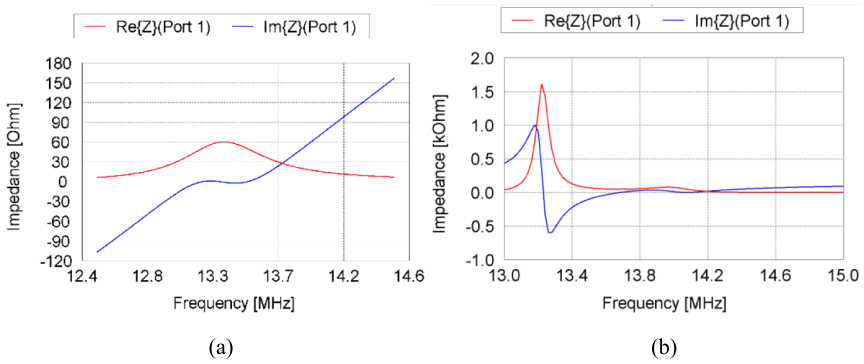


Fig. 8. Input impedance before and after optimization (a) The original WPT system (b) The optimized WPT system.

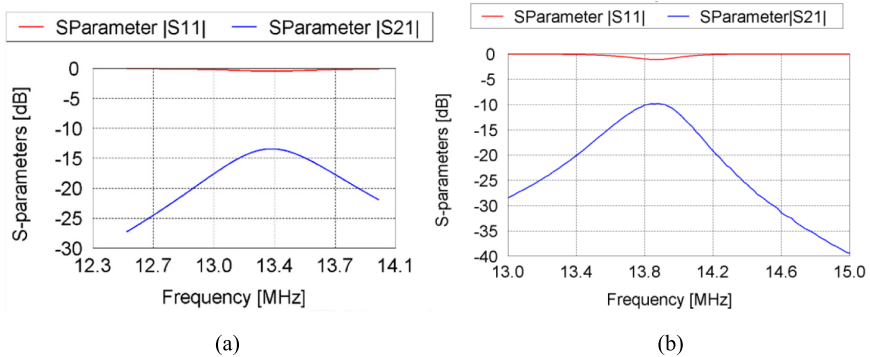


Fig. 9. S Parameter before and after optimization of 800 mm transmission distance (a) The original WPT system (b) The optimized WPT system.

Figure 9 (a) and (b) show the scattering parameter curves of the transmission system before and after optimization when the transmission distance is 1000 mm.

Compared with the 600 mm scattering parameter in Fig. 6, it can directly reflect the transmission performance of the system. When the transmission distance increases, the transmission performance of the system declines, but the decline speed of the unoptimized structure system is significantly faster than that of the optimized structure system.

At the resonance frequency $f = 14.1$ MHz and the load is matched to 50Ω , the initial distance between transmitting coil and receiving coil is 400 mm. The distance between the two coils is gradually increased in steps of 50 mm. Meanwhile, the value of compensation reactance X_i is adjusted to meet the matching conditions for each move. The corresponding values of the adjustment capacitance C_{eq} can be obtained by the Eqs. (18) and (21), and it varies curve with the transmission distance as shown in Fig. 10.

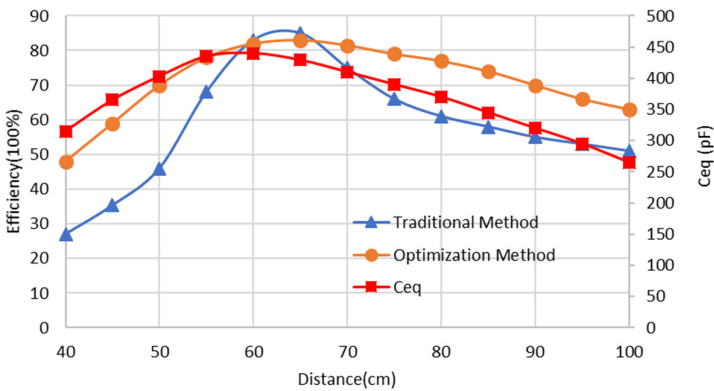


Fig. 10. The relationship between transmission efficiency and distance when $R_L = 50 \Omega$.

From Fig. 10, it can be observed that the measured power transmission efficiencies after matching is greatly improved, which proves the correctness of the above impedance matching theory. But at the best transmission distance, the transmission efficiency after compensation is lower than the original system. It is because that the loss of the external coupled transformation network at high frequency. The transmission distance and load voltage value of the measurement are recorded in the experiment. The corresponding efficiency values of the system at different transmission distances are calculated by simultaneous interpreting (5), (6) and (7).

When the load $R_L = 50 \Omega$ and coil distance $d = 60$ cm, the relationship between efficiency and frequency is shown in Fig. 11.

It can be seen from Fig. 11 that when the frequency changes, due to the existence of port impedance and external coupling, the system is out of tune, which greatly reduces the transmission efficiency of the system. By adding compensation reactance to the system for optimization, the matching capacitance C_{eq} is adjusted according to the impedance matching conditions when the frequency changes, so that it meets the

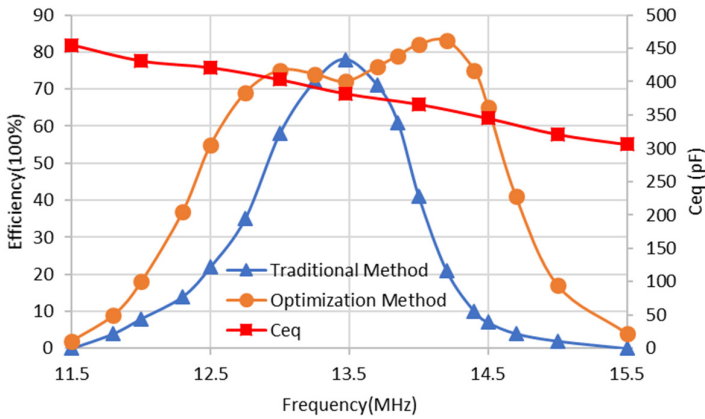


Fig. 11. The relationship between transmission efficiency and frequency when $R_L = 50 \Omega$.

relationship (12) and (13), the transmission efficiency of the optimized system is significantly improved, and the detuning is greatly improved. The efficiency between the two resonance frequency points of the optimized system will not decrease significantly, and it is far greater than the transmission efficiency of the system before optimization.

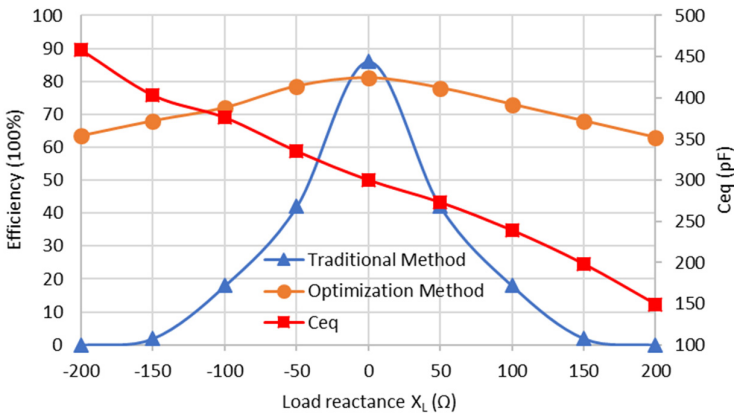


Fig. 12. The relationship between transmission efficiency and load reactance when $R_L = 50 \Omega$.

At the resonance frequency $f = 14.1 \text{ MHz}$, load $R_L = 50 \Omega$ and coil distance $d = 60 \text{ cm}$, the transmission efficiency of the WPT system decrease dramatically when the load reactance deviates from $X_L = 0 \Omega$ is shown in Fig. 12.

From Fig. 12, it can be observed that as the load reactance deviates from $X_i = 0$, the transmission efficiency of the system decreased rapidly with the inherent parameters of the system deviate from the resonant working frequency. By Adjusting the compensation capacitor C_{eq} to match the port impedance, the power transmission efficiency of

the WPT system can be significantly improved, but the resonance frequency will change.

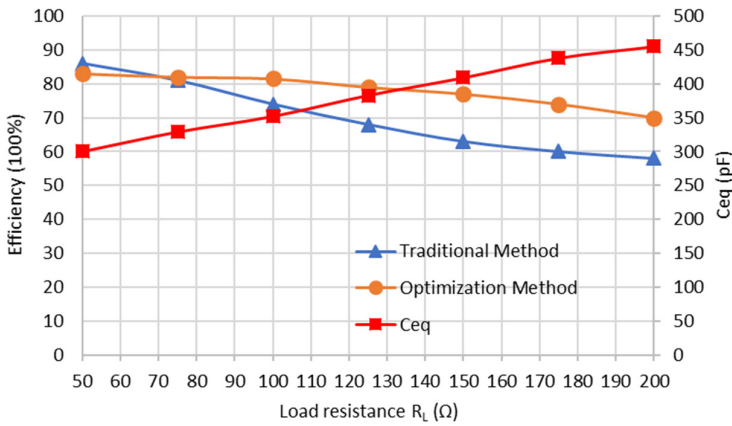


Fig. 13. The relationship between transmission efficiency and load resistance when $X_L = 0 \Omega$.

In Fig. 13, same operating conditions for transmission efficiency analysis when the load resistance deviates from $R_L = 50 \Omega$.

As shown in Fig. 13, the WPT system can maintain high power transmission efficiency even when the load resistance changes. Experimental results show that the proposed external coupling compensation matching method can significantly improve the robustness of WPT system when the load impedance changes.

5 Conclusions

This paper presents a new method to optimize the parameters of the system by using the external coupling network, designs the external coupling parameters and obtains the S-parameter model of the coupling matrix, which can simply use the magnetic coupling resonance model to represent the corresponding relationship between the ports and the resonance network, making the modeling of the complex multi-resonance magnetic coupling system simpler. We use frequency independent compensation reactance to match the detuning system, and get the conclusion that the transmission efficiency, resonance compensation and impedance matching of the system can be optimized by external coupling impedance transformation network. Simulation and experimental results show that the existence of external coupling network makes the port impedance match well, and the optimal value of external coupling at the maximum transmission efficiency is obtained.

Acknowledgments. This work was supported in part by the Natural Science Foundation of Liaoning Provincial under Grant 20180551056.

References

1. Shinohara, N.: Power without wires. *IEEE Microwave Mag.* **12**(7), 64–73 (2011)
2. Kurs, A.B., Karalis, A., Moffatt, R., Joannopoulos, J.D., Fisher, P., Soljacic, M.: Wireless power transfer via strongly coupled magnetic resonances. *Science* **317**(5834), 83–86 (2007)
3. Brown, W.C.: The history of power transmission by radio waves. *IEEE Trans. Microw. Theory Tech.* **32**(9), 1230–1242 (1984)
4. Ho, J.S., Kim, S., Poon, A.S.Y.: Midfield wireless powering for implantable systems. *Proc. IEEE* **101**(6), 1369–1378 (2013)
5. Waters, B.H., Smith, J.R., Bonde, P.: Innovative free-range resonant electrical energy delivery system (free-d system) for a ventricular assist device using wireless power. *ASAIO J.* **60**(1), 31–37 (2014)
6. Asgari, S.S., Bonde, P.: Implantable physiologic controller for left ventricular assist devices with telemetry capability. *J. Thoracic Cardiovasc. Surg.* **147**(1), 192–202 (2014)
7. Johari, R., Krogmeier, J.V., Love, D.J.: Analysis and practical considerations in implementing multiple transmitters for wireless power transfer via coupled magnetic resonance. *IEEE Trans. Ind. Electron.* **61**(4), 1774–1783 (2014)
8. Si, P., Hu, A.P., Malpas, S.C., Budgett, D.: A frequency control method for regulating wireless power to implantable devices. *IEEE Trans. Biomed. Circ. Syst.* **2**(1), 22–29 (2008)
9. Lee, K., Chae, S.H.: Effect of Quality Factor on Determining the Optimal Position of a Transmitter in Wireless Power Transfer Using a Relay. *IEEE Microw. Wirel. Compon. Lett.* **27**(5), 521–523 (2017)
10. Wei, X., Wang, Z., Dai, H.: A critical review of wireless power transfer via strongly coupled magnetic resonances. *Energies* **7**(7), 1–26 (2014)
11. Lin, Z., Wang, J., Fang, Z., Hu, M., Cai, C., Zhang, J.: Accurate maximum power tracking of wireless power transfer system based on simulated annealing algorithm. *IEEE Access* **6**, 60881–60890 (2018)
12. Li, W., Zhao, H., Li, S., Deng, J., Kan, T., Mi, C.C.: Integrated LCC compensation topology for wireless charger in electric and plug-in electric vehicles. *IEEE Trans. Ind. Electron.* **62**(7), 4215–4225 (2015)
13. Zhang, Y., Lu, T., Zhao, Z., Chen, K., He, F., Yuan, L.: Wireless power transfer to multiple loads over various distances using relay resonators. *IEEE Microw. Wirel. Compon. Lett.* **25**(5), 337–339 (2015)
14. Na, K., Jang, H., Ma, H., Bien, F.: Tracking optimal efficiency of magnetic resonance wireless power transfer system for biomedical capsule endoscopy. *IEEE Trans. Microw. Theory Tech.* **63**(1), 295–304 (2015)
15. Anowar, T.I., Barman, S.D., Wasif Reza, A., Kumar, N.: High-efficiency resonant coupled wireless power transfer via tunable impedance matching. *Int. J. Electron.* **104**(10), 1607–1625 (2017)
16. Miao, Z., Liu, D., Gong, C.: Efficiency enhancement for an inductive wireless power transfer system by optimizing the impedance matching networks. *IEEE Trans. Biomed. Circ. Syst.* **11**(5), 1160–1170 (2017)
17. Nguyen, H., Agbinya, J.I.: Splitting frequency diversity in wireless power transmission. *IEEE Trans. Power Electron.* **30**(11), 6088–6096 (2015)
18. Berger, A., Agostinelli, M., Vesti, S., Oliver, J.A., Cobos, J.A., Huemer, M.: A wireless charging system applying phase-shift and amplitude control to maximize efficiency and extractable power. *IEEE Trans. Power Electron.* **30**(11), 6338–6348 (2015)

19. Lim, Y., Tang, H., Lim, S., Park, J.: An adaptive impedance-matching network based on a novel capacitor matrix for wireless power transfer. *IEEE Trans. Power Electron.* **29**(8), 4403–4413 (2014)
20. Beh, T.C., Kato, M., Imura, T., Oh, S., Hori, Y.: Automated impedance matching system for robust wireless power transfer via magnetic resonance coupling. *IEEE Trans. Ind. Electron.* **60**(9), 3689–3698 (2013)
21. Kim, J., Kim, D.H., Park, Y.J.: Analysis of capacitive impedance matching networks for simultaneous wireless power transfer to multiple devices. *Ind. Electron. IEEE Trans.* **62**(5), 2807–2813 (2015)
22. Kim, J., Jeong, J.: Range-adaptive wireless power transfer using multiloop and tunable matching techniques. *Ind. Electron. IEEE Trans.* **62**(10), 6233–6241 (2015)
23. Kim, J., Kim, D.H., Park, Y.J.: Free-positioning wireless power transfer to multiple devices using a planar transmitting coil and switchable impedance matching networks. *IEEE Trans. Microw. Theory Tech.* **64**(11), 3714–3722 (2016)
24. Miao, Z., Liu, D., Gong, C.: An adaptive impedance matching network with closed loop control algorithm for inductive wireless power transfer. *Sensors* **17**(8), 1759–1778 (2017)
25. Bito, J., Jeong, S., Tentzeris, M.M.: A novel heuristic passive and active matching circuit design method for wireless power transfer to moving objects. *Microw. Theory Tech. IEEE Trans.* on **65**(4), 1094–1102 (2017)